Electronic Supplementary Material (ESI) for Energy & Environmental Science.

Electronic Supplementary Information

High-performance Flexible Asymmetric Supercapacitors Based on A New Graphene Foam/Carbon Nanotubes Hybrid Film

Jilei Liu,[abc] *Lili Zhang,*[b] *Hao Bin Wu,*[c] *Jianyi Lin,*[ab] *Zexiang Shen,**[a] *and Xiong Wen (David) Lou**[c]

[a] Division of Physics and Applied Physics, School of Physical and Mathematical Sciences, Nanyang Technological University, 21 Nanyang link, Singapore 637371 Email: zhexiang@ntu.edu.sg

[b] Heterogeneous Catalysis, Institute of Chemical Engineering and Sciences, A*Star, 1 Pesek Road, Jurong Island, Singapore 627833

[c] School of Chemical and Biomedical Engineering, Nanyang Technological University, 62 Nanyang Drive, Singapore 637459

Email: xwlou@ntu.edu.sg or davidlou88@gmail.com; webpage: http://www.ntu.edu.sg/home/xwlou/

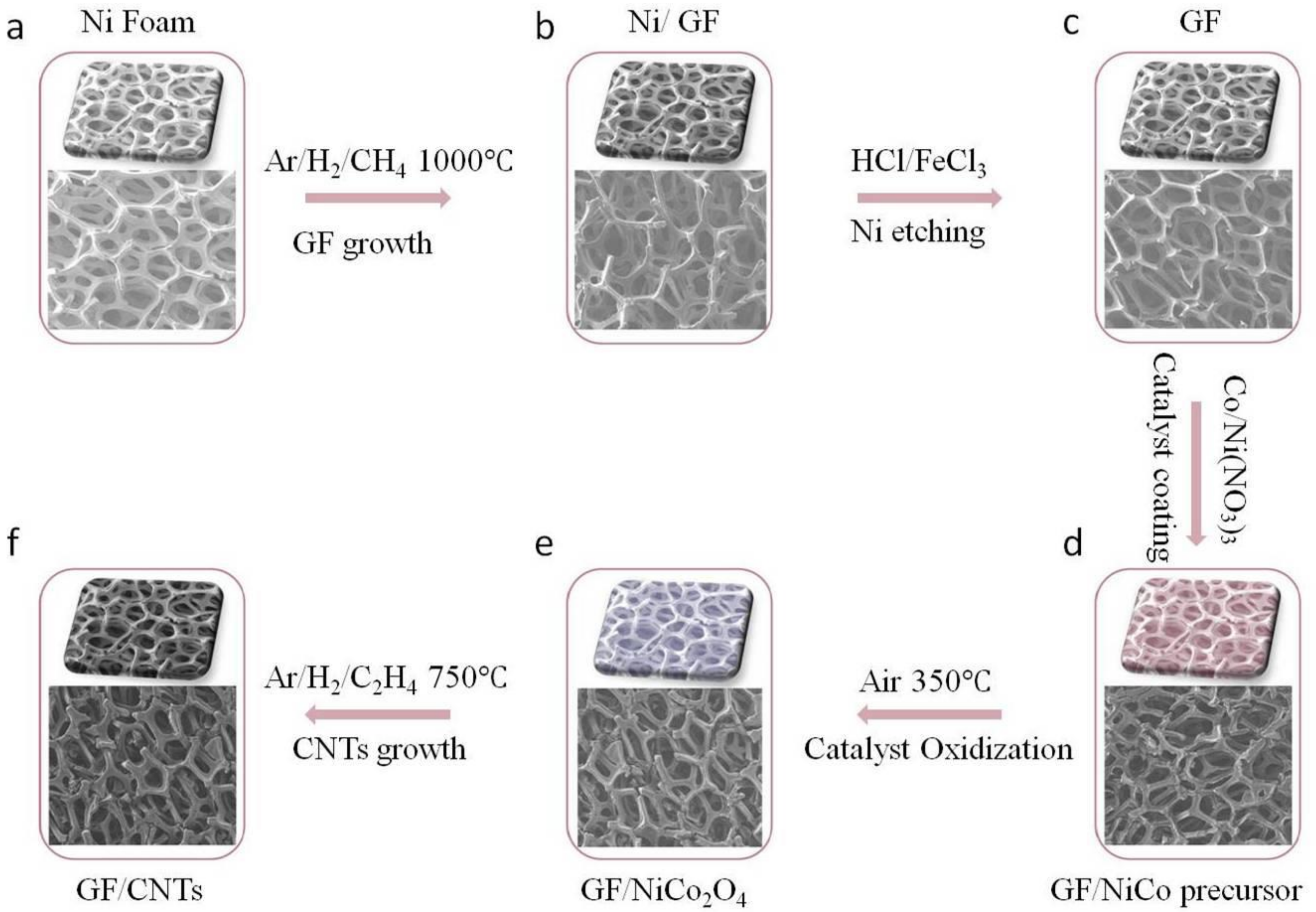

Fig. S1 Illustration of the growth procedure of GF/CNTs hybrid films. (**a**) Ni foam substrate; (**b**) direct growth of graphene films on nickel foam via CH_4 decomposition; (**c**) removal of Ni network to form free-standing graphene foam (GF); (**d**) deposition of NiCo-precursor on the GF via a hydrothermal method; (**e**) conversion of GF/NiCo-precursor to GF/$NiCo_2O_4$; (**f**) growth of carbon nanotubes onto GF at 750 ^{o}C in the presence of H_2 and C_2H_4 using the Ni-Co-O catalyst, forming 3D GF/CNTs hybrid structure.

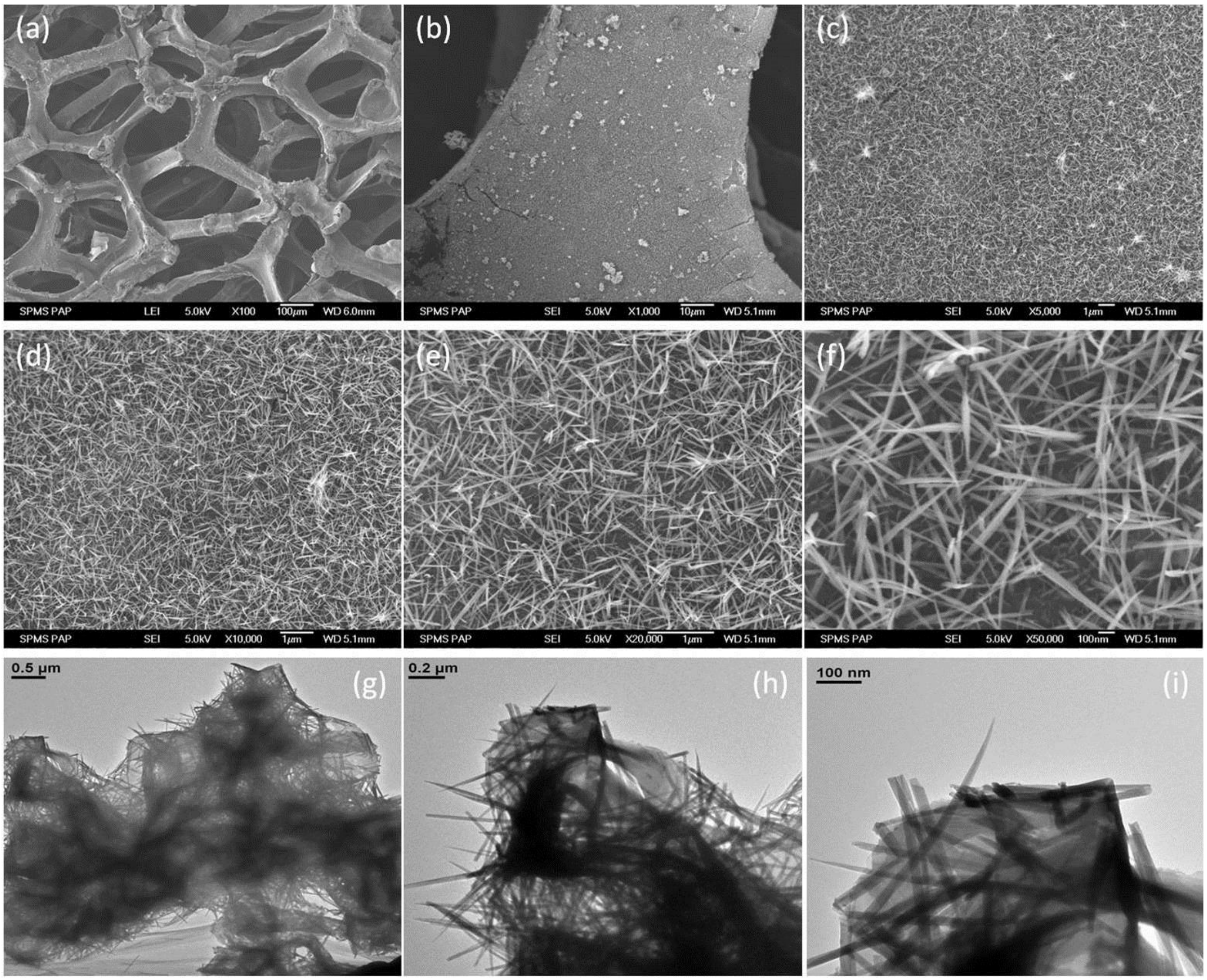

Fig. S2 (a-f) Typical FESEM and (g-i) TEM images of the GF/$NiCo_2O_4$ hybrid film.

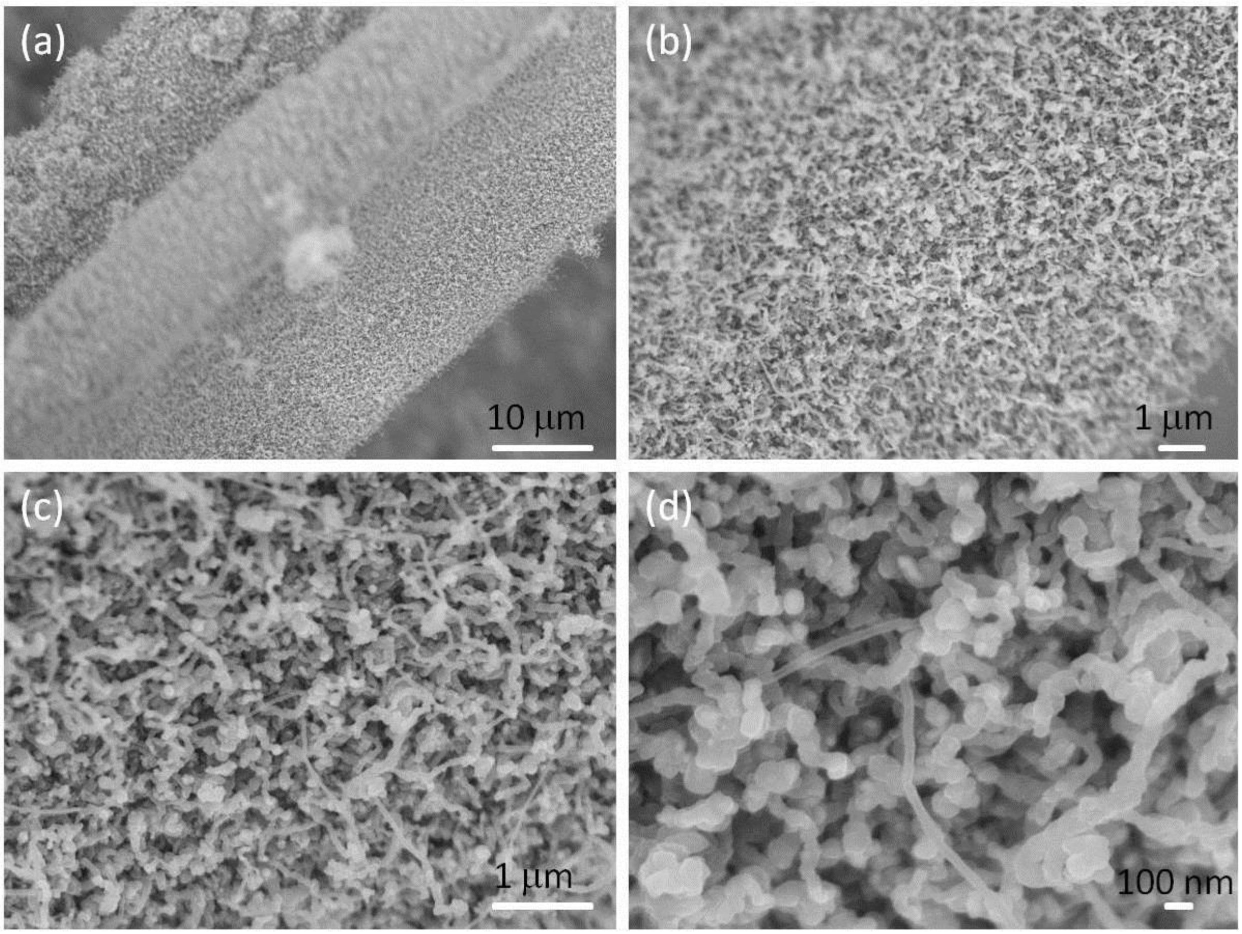

Fig. S3 FESEM images of GF/CNTs hybrid film using a conventional dip-coating method to load NiCo catalysts.

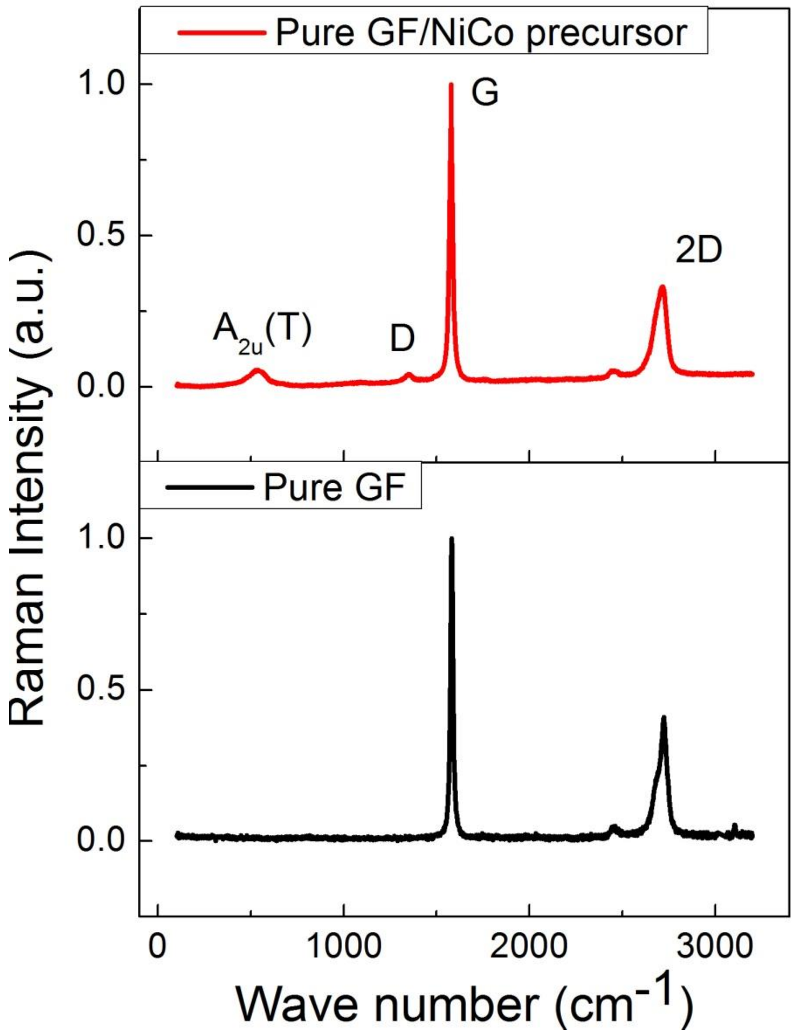

Fig. S4 Comparative Raman spectrums of the pure GF before and after NiCo precursor coating. The peak A_{2u} (T) at about 515 cm^{-1} is attribute to the formation of NiCo precursor.[1] The low intensity of D band for GF/NiCo precursor hybrid film suggests that only a few defects were introduced during catalyst loading process.[2]

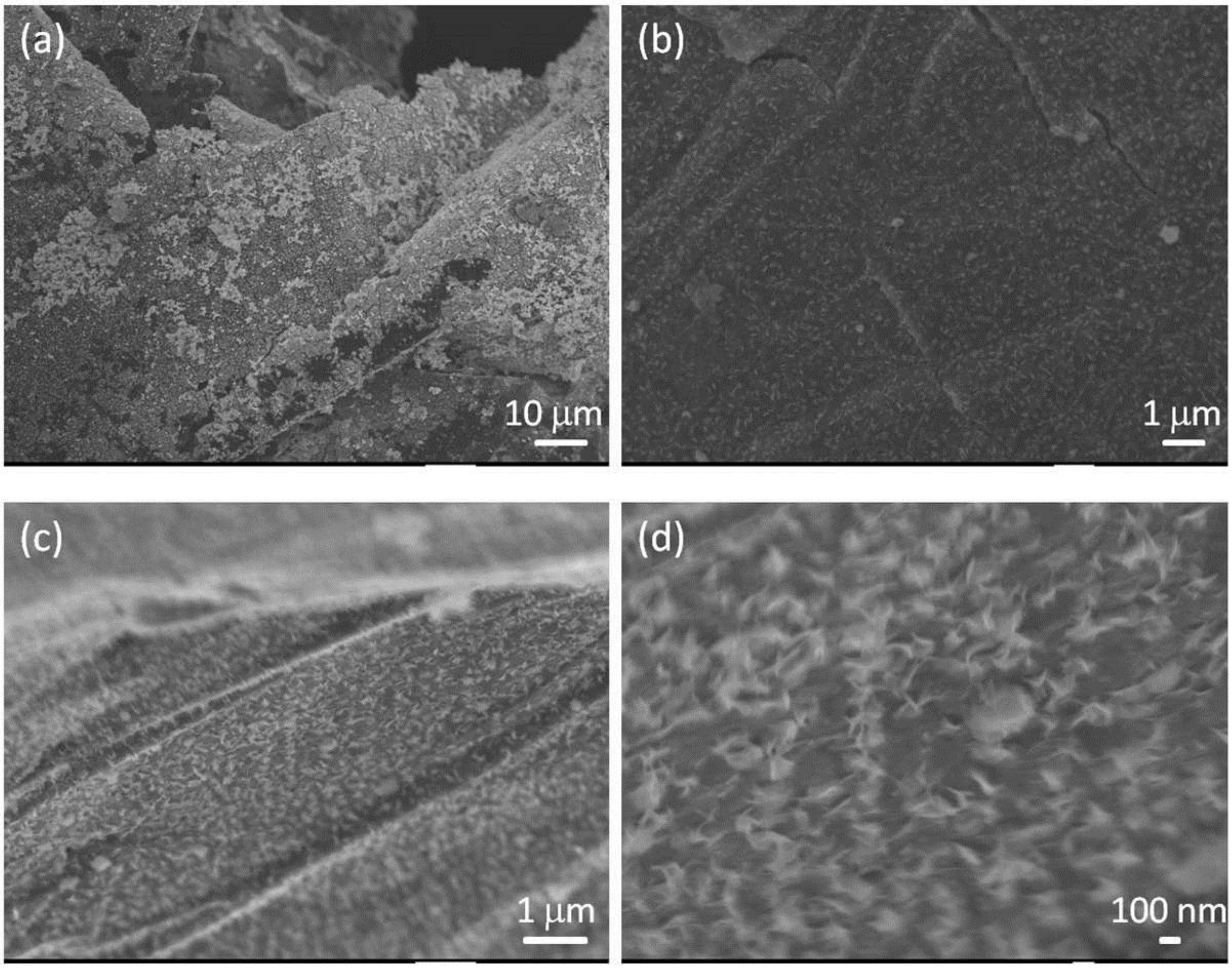

Fig. S5 Typical FESEM images of the GF/$NiCo_2O_4$ hybrid film after annealed in H_2 atmosphere at 350 ^{o}C for 0.5 h. The formation of catalyst islands is clearly observed.

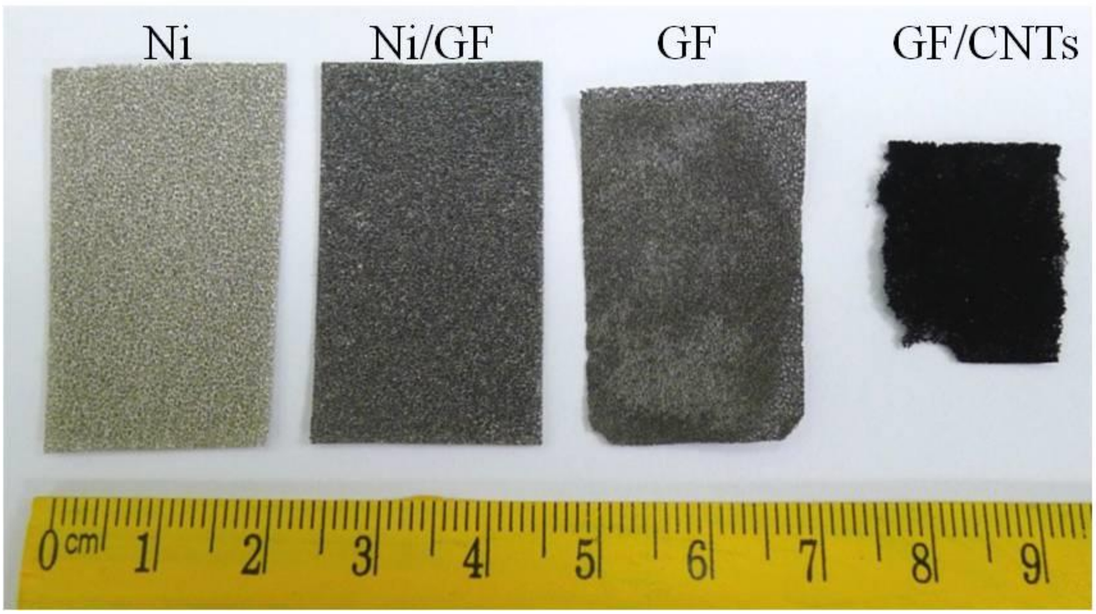

Fig. S6 Optical images of inch-scaled nickel foam (Ni), Ni/GF, GF, and GF/CNTs.

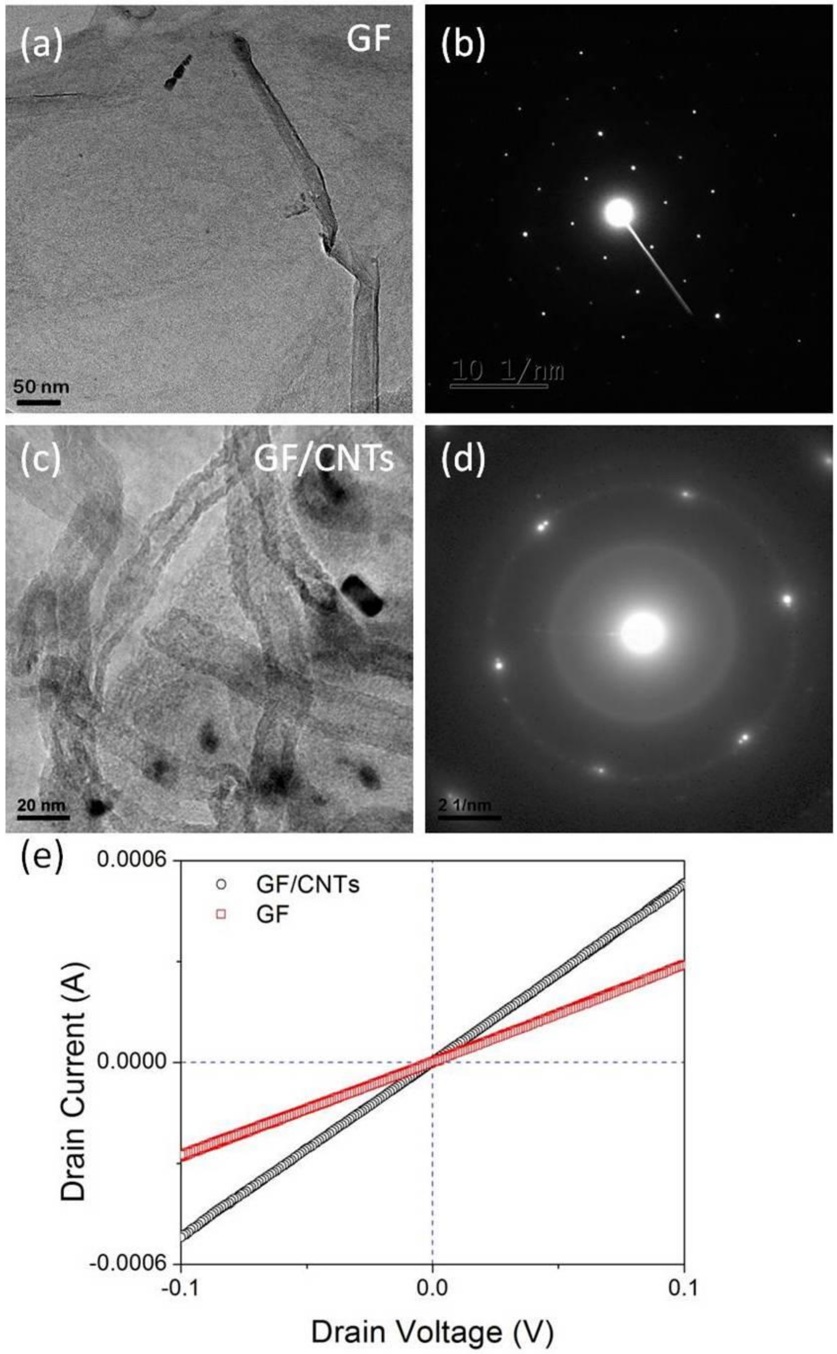

Fig. S7 Typical TEM images of pure GF (a), GF/CNTs(c) and their corresponding selected area electron diffraction patterns (b) and (d), respectively. (e) Comparative I-V curves of pure GF (thickness of 28 μm) and GF/CNTs hybrid film (thickness of 29 μm). Corresponding conductance were measured to be 101 S/m for GF and 178 S/m for GF/CNTs hybrid film.

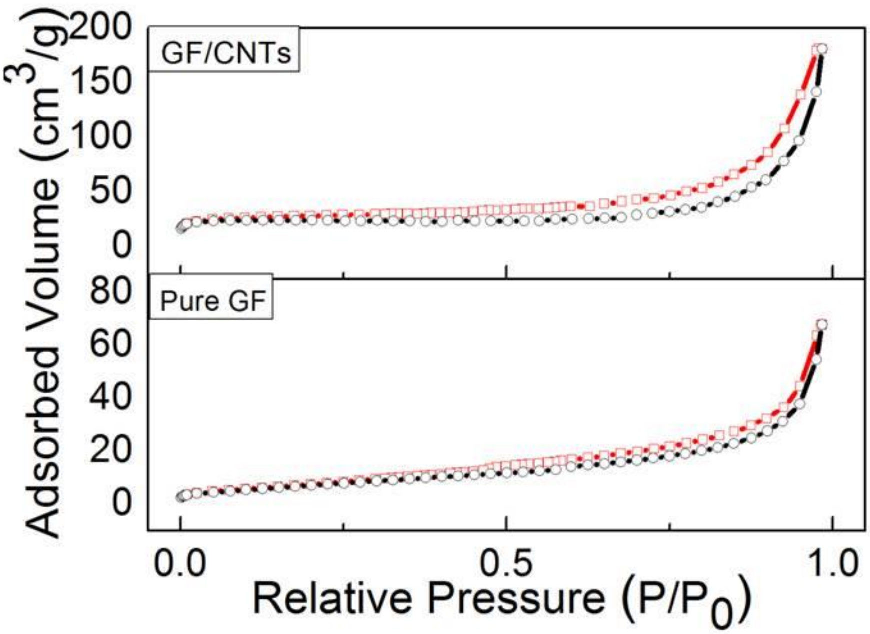

Fig. S8 N_2 adsorption/desorption isotherms of pure GF and GF/CNTs hybrid film.

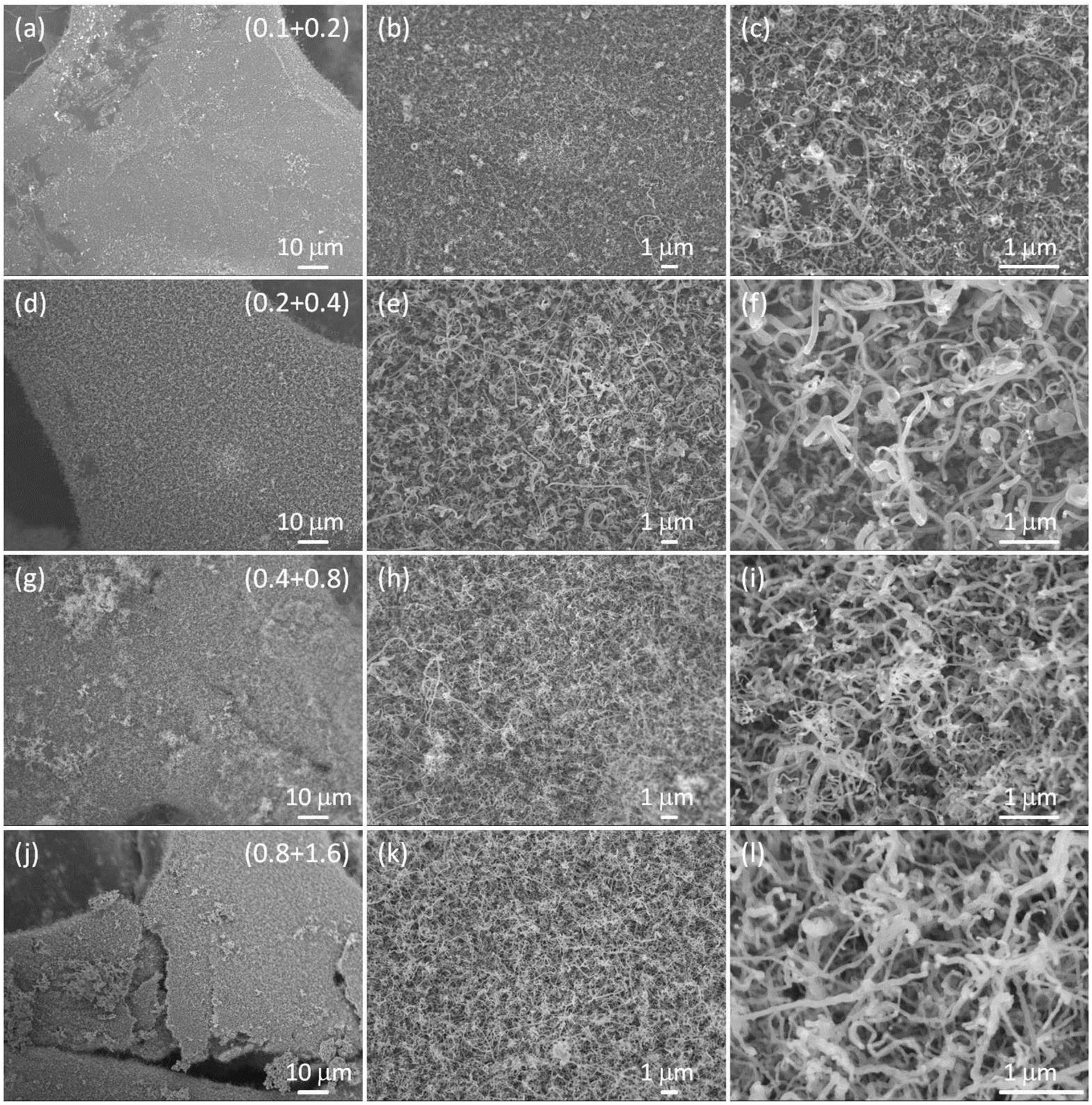

Fig. S9 Typical FESEM images of GF/CNTs hybrid films with different loading amounts of CNTs at different magnifications. The numbers in the first column indicate the added amount of Ni, Co sources (mmol, see Method section).

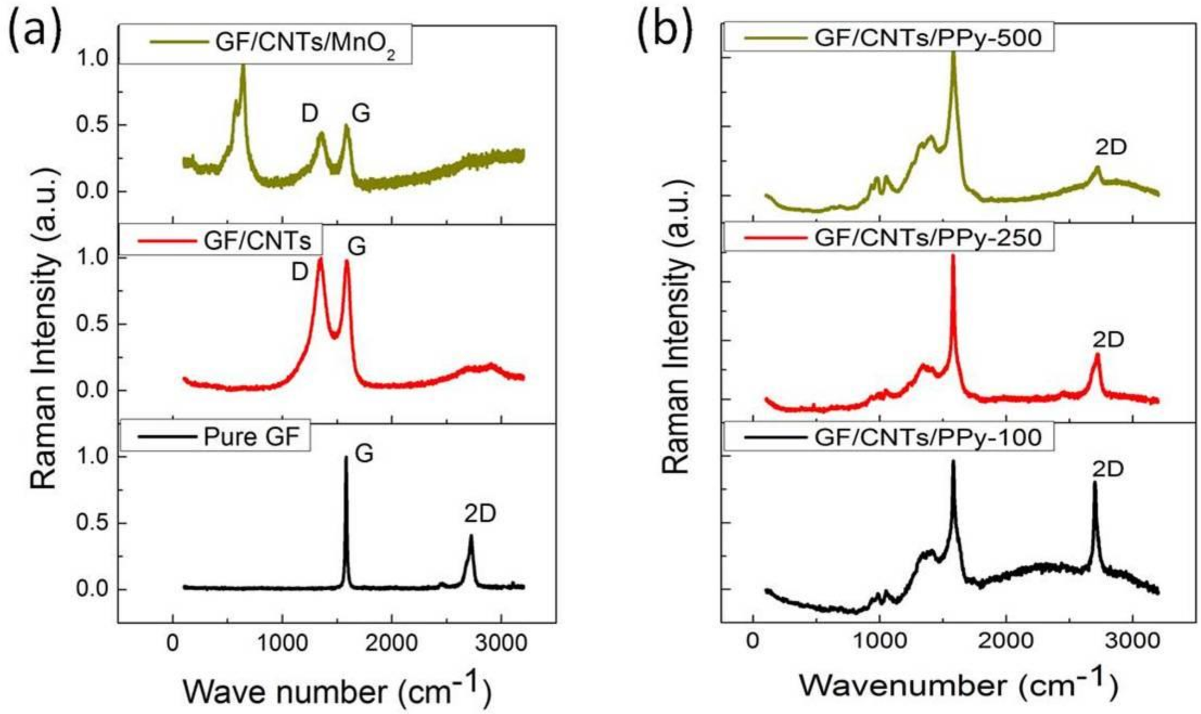

Fig. S10 (a) Raman spectra of GF/CNTs/MnO_2, GF/CNTs and pure GF. (b) Raman spectra for GF/CNTs/Ppy hybrid films with different loading of Ppy. The appearance of typical MnO_2 Raman peaks at 491 cm^{-1}, 568 cm^{-1}, 640 cm^{-1} as well as the decrease in intensity of G band further verifies the successful deposition of MnO_2.[3] The appearance of characteristic Raman peaks at 980 cm^{-1} and 1045 cm^{-1} suggests the polymerization of Ppy.[4]

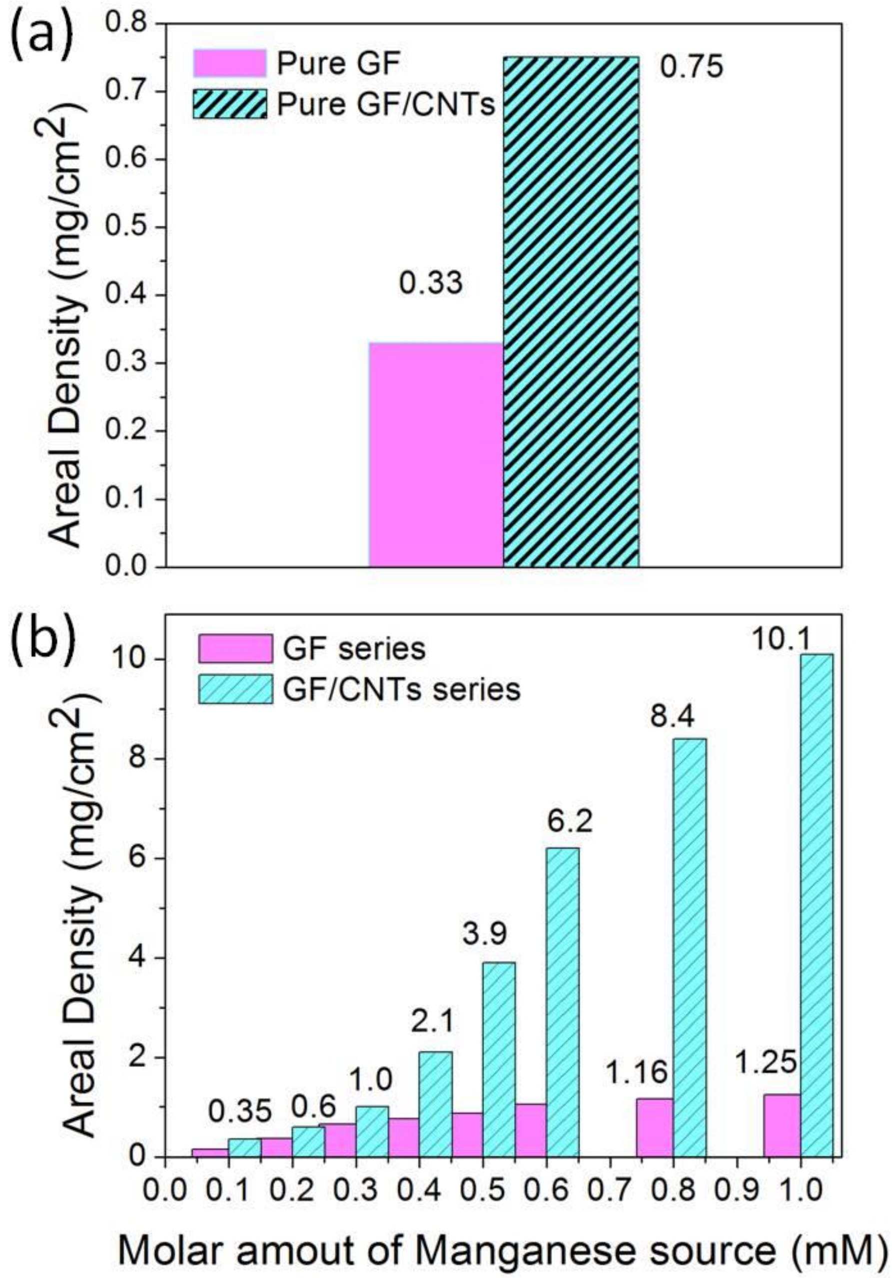

Fig. S11 (a) Areal density of pure GF and GF/CNTs films. (b) Areal density of loaded active materials (MnO_2) for GF and GF/CNTs with manganese source concentration from 0.1 to 1 mM.

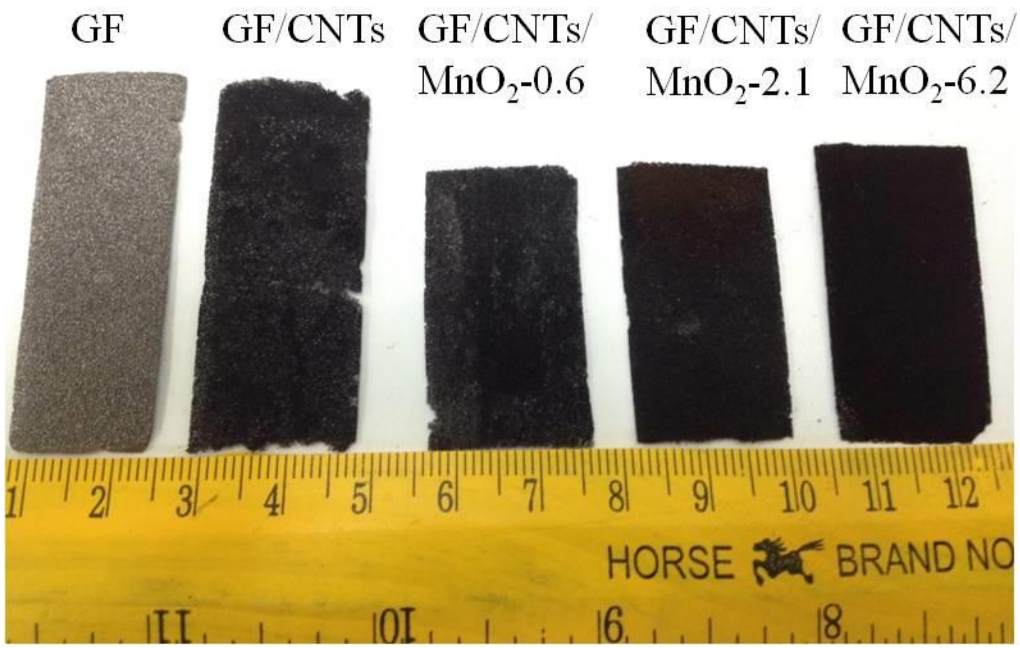

Fig. S12 Optical image of inch-scaled pure graphene foam (GF), GF/CNTs, GF/CNTs/MnO_2-0.6, GF/CNTs/MnO_2-2.1 and GF/CNTs/MnO_2-6.2.

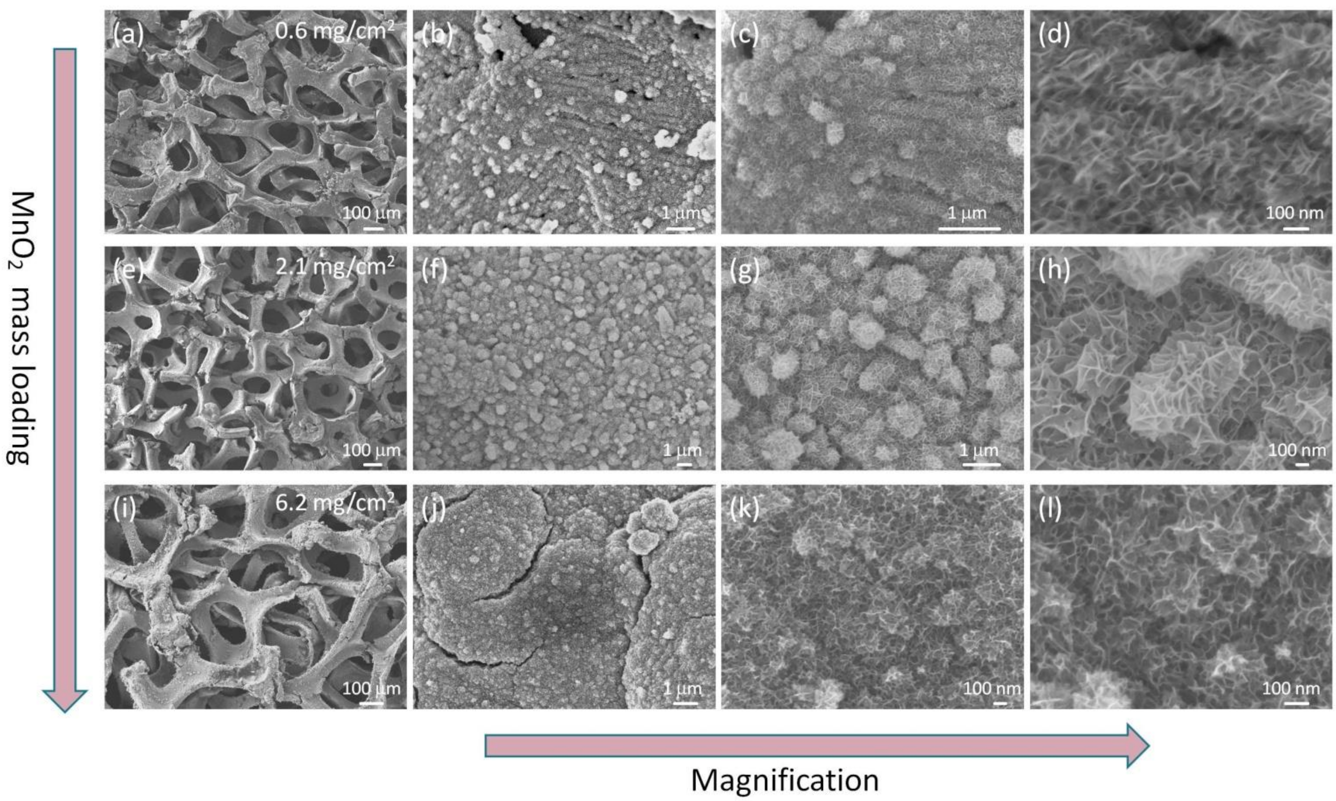

Fig. S13 Typical FESEM images of GF/CNTs/MnO_2 hybrid films with different loading amount of MnO_2 at different magnifications.

Table S1. Fitting results for Electrochemical Impedance Spectroscopy

	Samples	R_s (Ω)	R_{ct} (Ω)	W	CPE
GF/CNTs/MnO_2	0.6	7.4	5.6	0.61679	0.86972
	1.0	7.5	12.2	0.61883	0.86416
	2.1	8.3	21.9	0.87347	0.67988
	3.9	8.9	23.5	0.54721	0.63146
	6.2	7.1	31.6	0.60841	0.52994
	8.4	8.3	56.2	0.78084	0.63544
GF/CNTs/Ppy	100	7.6	6.9	0.68548	0.62276
	250	7.5	6.1	0.74289	0.63634
	500	7.0	5.2	0.83395	0.55705
	1000	8.3	10.7	0.63947	0.57515
	1500	7.2	22.6	0.59736	0.72990
	2000	8.1	28.6	0.79936	0.70254
ASCs	0.6	1.6	16.1	0.76437	0.37655
	2.1	6.4	20.0	0.74294	0.68914

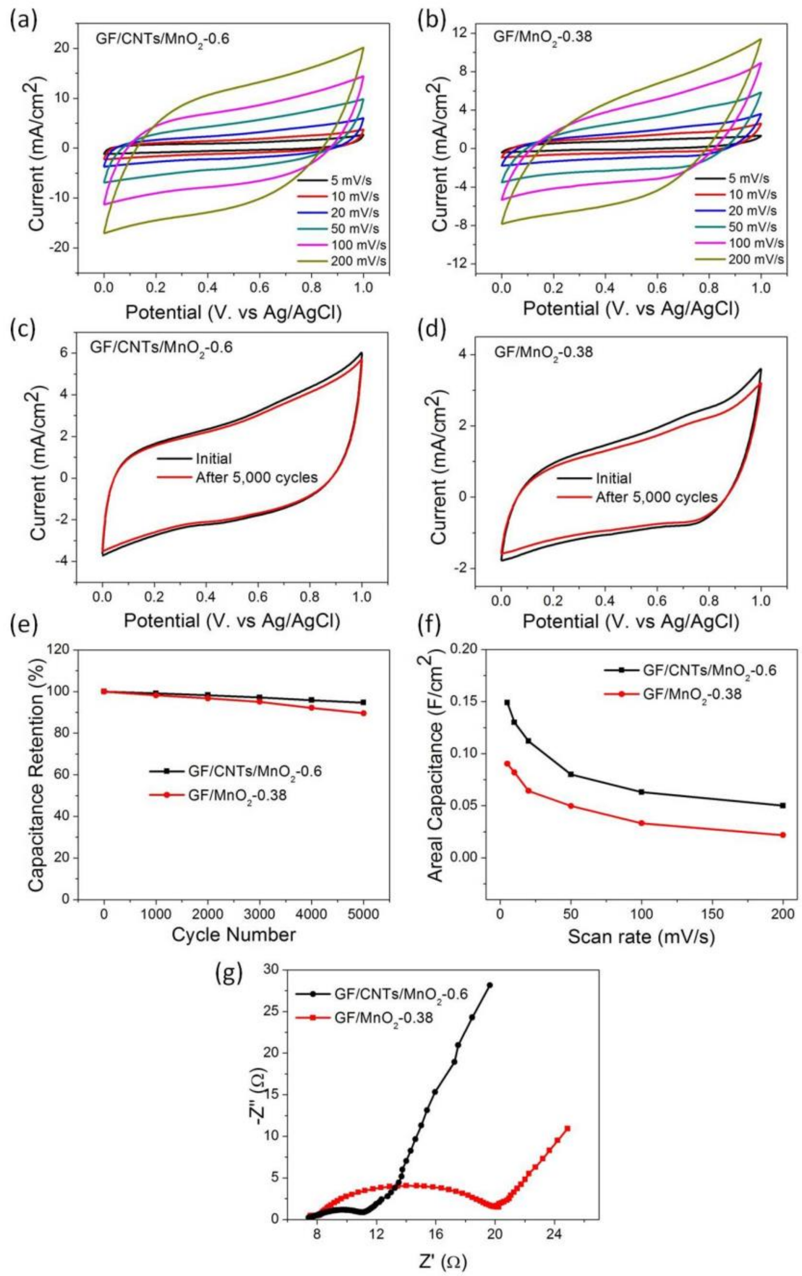

Fig. S14 CV curves of GF/CNTs/MnO_2-0.6 hybrid film (a) and GF/MnO_2-0.38 (b) at various scan rates (from 5 to 200 mV/s). Comparative CV curves of GF/CNTs/MnO_2-0.6 hybrid film (c) and GF/MnO_2-0.38 (d) at a scan rate of 20 mV/s before and after 5,000 cycles and the corresponding capacitance retention plot up to 5, 000 cycles (e). (f) Comparative areal capacitances vs. scan rate. (g) Comparative electrochemical impedance spectroscopy. The R_{ct} for GF/CNTs/MnO_2-0.6 is 5.6 Ω, which is smaller than that of GF/MnO_2-0.38 (13 Ω).

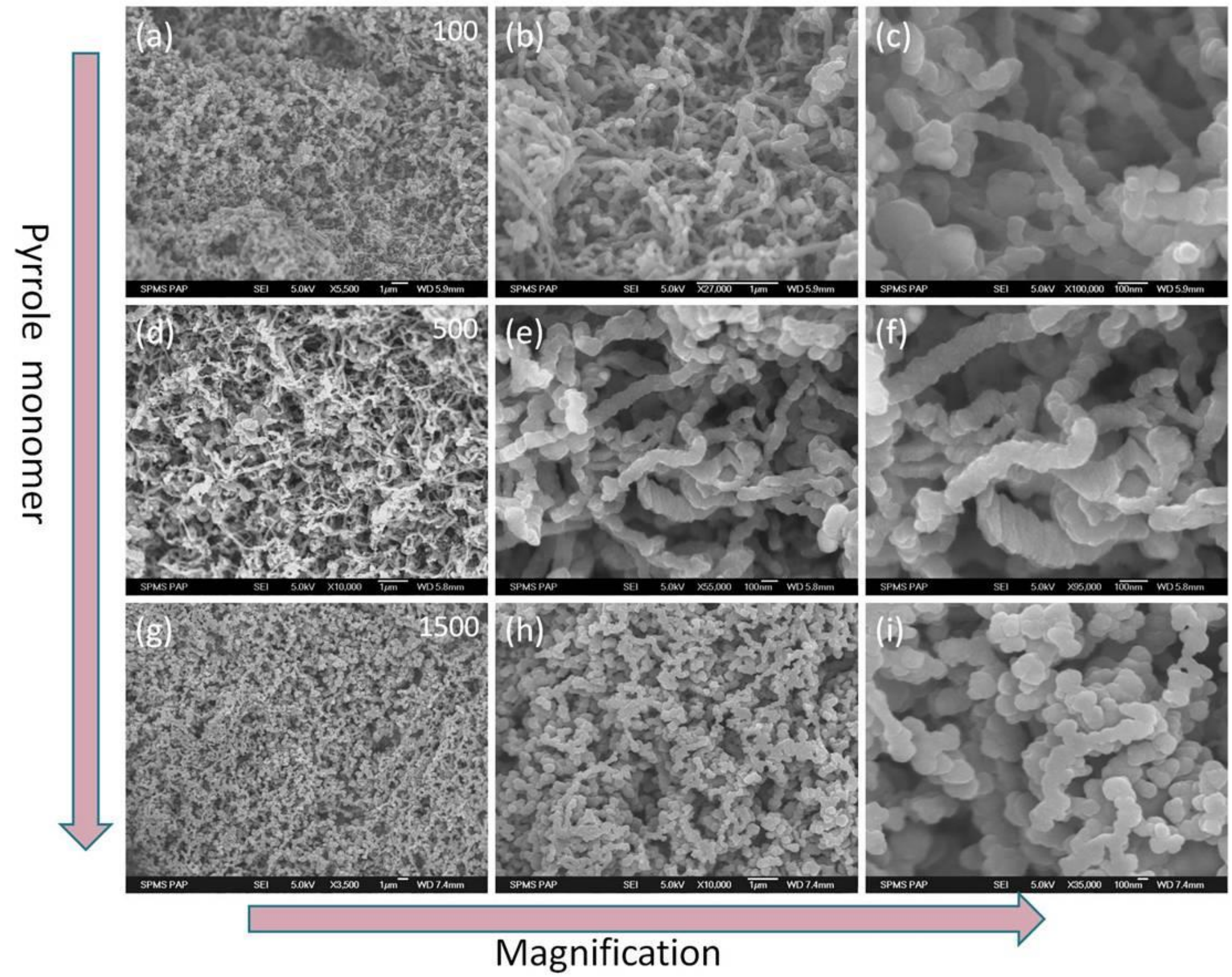

Fig. S15 Typical FESEM images of GF/CNTs/Ppy hybrid films with different amount of monomer at different magnifications.

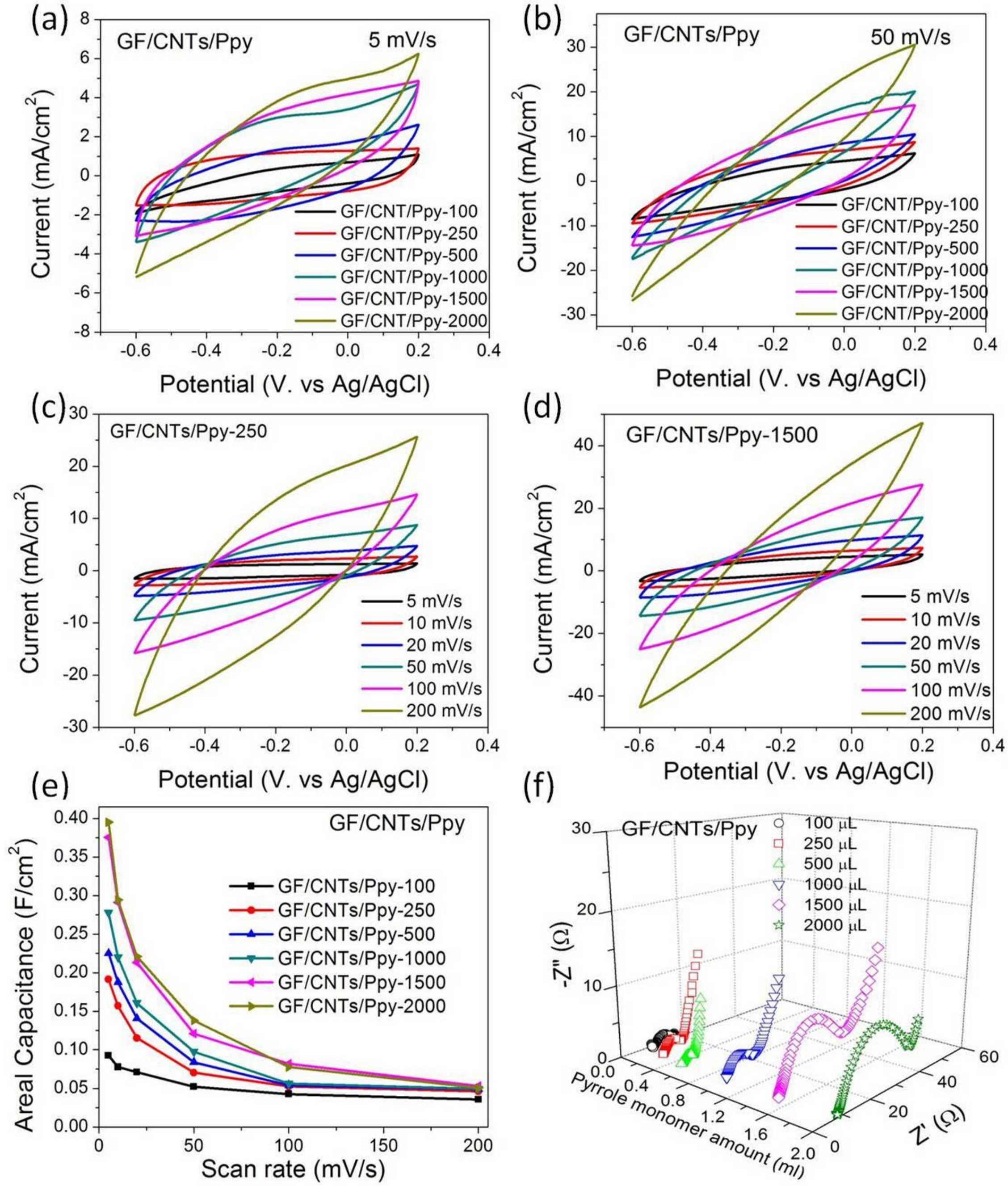

Fig. S16 Comparative CV curves of GF/CNTs/Ppy hybrid films at scan rates of (a) 5 mV/s and (b) 50 mV/s. CV curves for (c) GF/CNTs/Ppy-250 and (d) GF/CNTs/Ppy-1500 measured at different scan rates. (e) Areal capacitance of GF/CNTs/Ppy hybrid films as a function of scan rate. (f) Nyquist plots of the GF/CNTs/Ppy hybrid films.

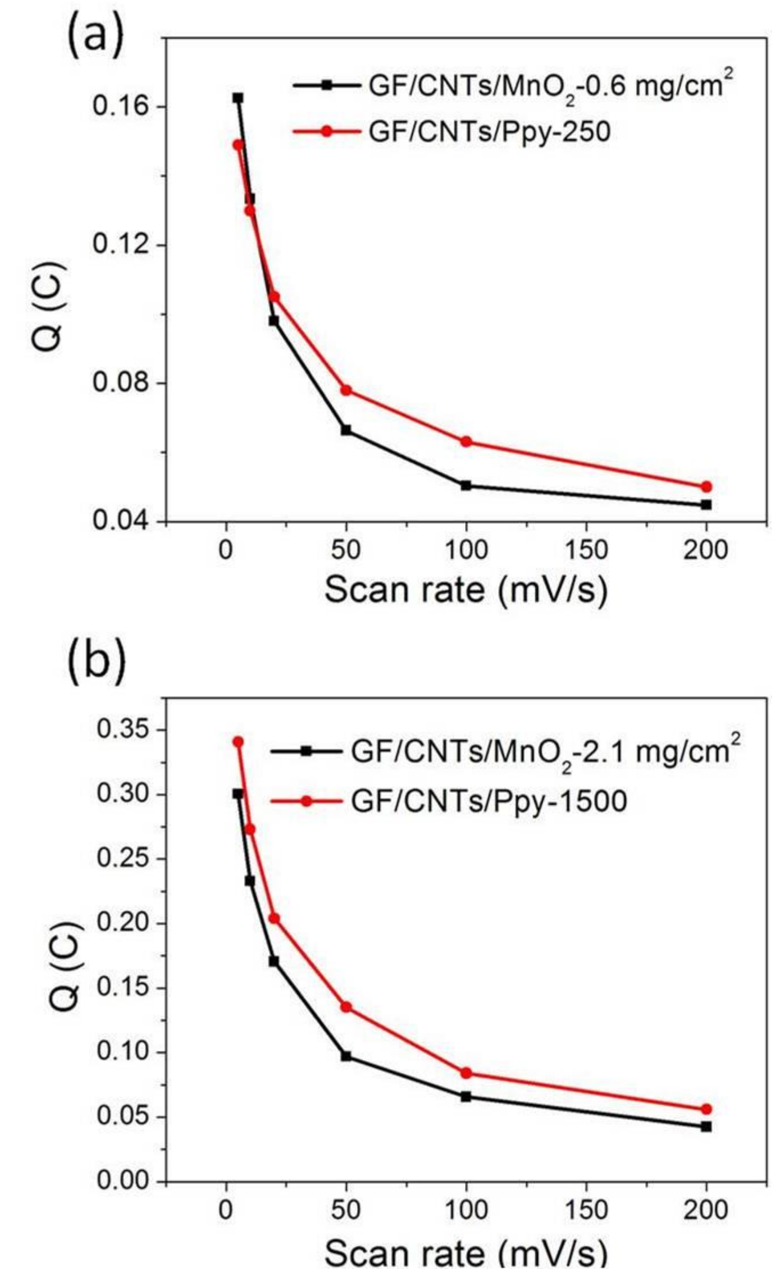

Fig. S17 Charge balance of two couples of electrodes.

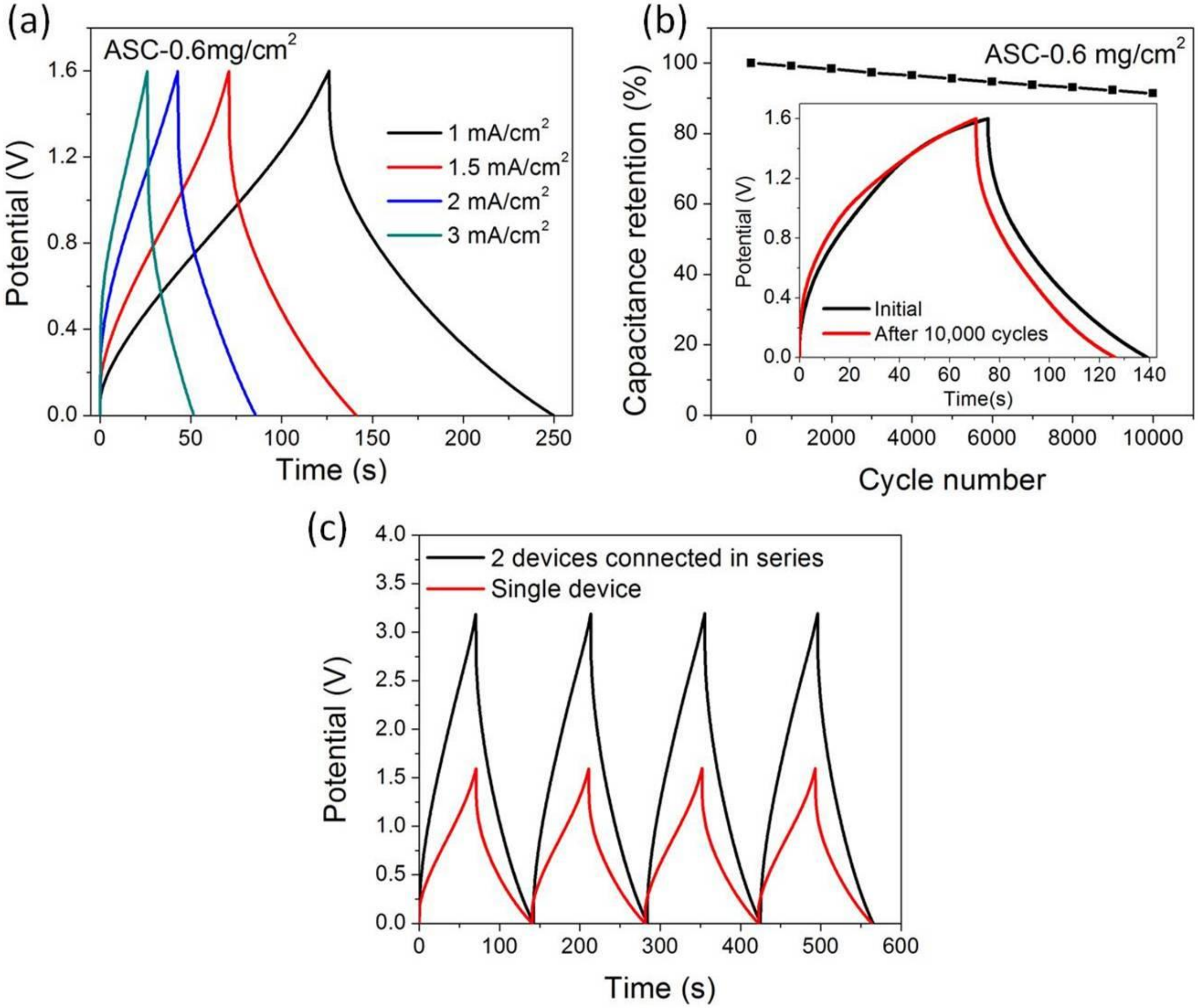

Fig. S18 (a) Galvanostatic charge/discharge curves of ASC-0.6 at different current densities. (b) Cycling performance of ASC-0.6 at a current density of 1.5 mA/cm^2 for 10000 cycles. Inset shows the charge/discharge curves for the 1st and 10000th cycles. (c) Galvanostatic charge/discharge curves for two ASC-0.6 devices connected in series (with an output voltage of 3.2 V). Charge/discharge curves of a single ASC is also shown for comparison. Both of them are collected at a current density of 1.5 mA/cm^2.

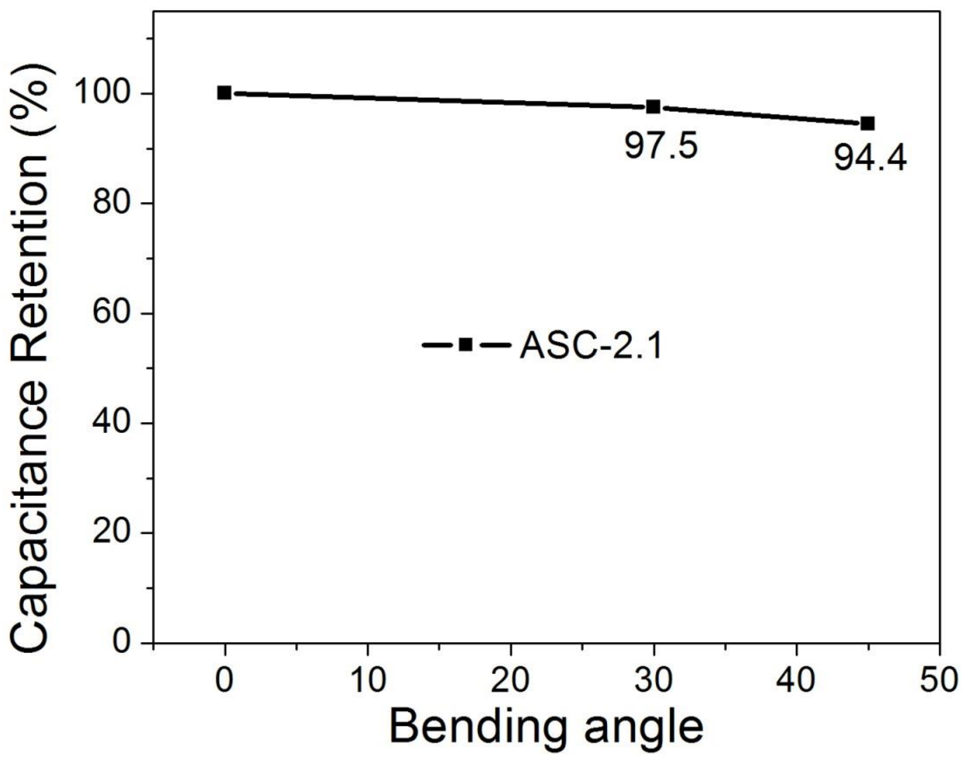

Fig. S19 Specific capacitance vs. bending angle for ASC-2.1.

Table S2. Parameters for the asymmetric supercapacitors (ASCs) and the calculated volumetric and gravimetric energy/power densities based on the fully packaged cell.

		Thickness (μm)	Density (g/cm^3)	Weight percentage	Volume percentage
ASC-0.6	Positive Electrode (GF/CNTs/MnO_2-0.6)	**33**	**0.41**	**28.5**	**35.9**
	Negative Electrode (GF/CNTs/Ppy-250)	**30**	**0.42**	**26.4**	**32.6**
	Separator	**29**	**0.39**	**23.9**	**31.5**
	Electrolyte (0.5 M Na_2SO_4)	**-**	**1.06**	**21.2**	**-**
ASC-2.1	Positive Electrode (GF/CNTs/MnO_2-2.1)	**36**	**0.79**	**38.9**	**37.1**
	Negative Electrode (GF/CNTs/Ppy-1000)	**32**	**0.75**	**32.1**	**33**
	Separator	**29**	**0.39**	**15.4**	**29.9**
	Electrolyte (0.5 M Na_2SO_4)	**-**	**1.06**	**13.6**	**-**
		E_{max} (Wh/kg)	P_{max} (kW/kg)	E_{max} (Wh/L)	P_{max} (kW/L)
ASC-0.6	Active materials (MnO_2+Ppy)	**22.2**	**10.3**	**-**	**-**
	Electrodes (including GF/CNTs films)	**9.4**	**4.4**	**3.9**	**1.8**
	Full Cell	**5.2**	**2.4**	**2.7**	**1.2**
ASC-2.1	Active materials (MnO_2+Ppy)	**22.8**	**2.7**	**-**	**-**
	Electrodes (including GF/CNTs films)	**16.2**	**1.9**	**12.5**	**1.5**
	Full Cell	**11.5**	**1.3**	**8.7**	**1.0**

Remarks: The electrolyte is absorbed by the electrodes and thus does not take up any volume in the packaged cell.

For ASC-0.6: total cell mass is 18.8 mg; total volume is 36.8 μL; density of packaged cell is 0.51 g/cm^3.

For ASC-2.1: total cell mass is 29.3 mg; total volume is 38.4 μL; density of packaged cell is 0.76 g/cm^3.

Reference

1. Audemer, A., Delahaye, A., Farhi, R., Sac-Epée, N. & Tarascon, J. M. Electrochemical and Raman Studies of Beta-Type Nickel Hydroxides $Ni_{1-x}Co_x(OH)_2$ Electrode Materials. *J. Electrochem. Soc.* **144**, 2614-2620 (1997).
2. Dimiev, A. *et al.* Layer-by-Layer Removal of Graphene for Device Patterning. *Science* **331**, 1168-1172 (2011).
3. Gao, T., Fjellvåg, H. & Norby, P. A comparison study on Raman scattering properties of α- and β-MnO_2. *Anal. Chim. Acta* **648**, 235-239 (2009).
4. Le, H. N. T., Bernard, M. C., Garcia-Renaud, B. & Deslouis, C. Raman spectroscopy analysis of polypyrrole films as protective coatings on iron. *Synth. Met.* **140**, 287-293 (2004).